Star clusters: basic galactic building blocks
Proceedings IAU Symposium No. 266, 2009
R. de Grijs & J. R. D. Lépine, eds.

doi:10.1017/S1743921309991943

Astrometry and photometry of stars and star clusters in M33

Izaskun San Roman,[1] Ata Sarajedini,[1] Carme Gallart[2] and Antonio Aparicio[2]

[1]Department of Astronomy, University of Florida, 211 Bryant Space Science Center, Gainesville, FL 32611-2055, USA
email: [izaskun, ata]@astro.ufl.edu

[2]Instituto de Astrofísica de Canarias, Vía Láctea, s/n, E38200 La Laguna, Tenerife, Spain

Abstract. We present positions and magnitudes of stars and star clusters in a $1^\circ \times 1^\circ$ area centered on M33. The survey is based on deep archival ground-based images using the MegaPrime camera on the 3.6m *Canada–France–Hawaii telescope*. We provide u', g', r', i', z' magnitudes by performing standard profile-fitting photometry of these images and apply image classification algorithms such as SExtractor. We also present a catalog of extended sources by applying visual-inspection classification. This complete catalog provides promising targets for deep photometry with *HST* and for high-resolution spectroscopy to study the structure and star-formation history of the disk and halo of M33.

Keywords. galaxies: individual (M 33), galaxies: spiral, galaxies: star clusters, galaxies: stellar content

1. Introduction

The diverse set of issues required to understand the formation history of a galaxy involves the need for a comprehensive study of its stars and star clusters. In particular, the ages, metallicities and kinematics of star clusters are representative of the galaxy-formation process. These correlations underscore the importance of compiling complete catalogs of stars and star clusters in nearby galaxies. At a distance of ~ 870 kpc, M33 is the only nearby late-type spiral galaxy providing a connection between the cluster populations of earlier-type spirals and the numerous, nearby later-type dwarf galaxies. An up-to-date catalog of star clusters in M33 can be found in Sarajedini & Mancone (2007; SM hereafter) who merged all modern catalogs of star clusters and cluster candidates. However, as discussed by the authors, the sample of clusters suffer from severe incompleteness. A more recent catalog produced by Zloczewski *et al.* 2008 (hereafter ZKH) was derived from the same data used in this study. They present a catalog of 4780 extended sources, including 3554 new candidate stellar clusters. While employing a comparable method, we achieve somewhat different results.

2. Observations and reduction

Processing of the CCD frames was performed as a part of the *CFHT* Queue Service Observing Mode using the ELIXIR pipeline. To facilitate the search of objects, only the best images available were analyzed, consisting of 15 g', 14 r', 15 u', 28 i' and 3 z' with median seeing values of $< 0.8''$ in g', r' and i' and $\sim 0.6''$ in u' and z'. We divided each final, combined image into two subfields, including an overlapping area, to deal with the spatial variability of the point-spread function (PSF).

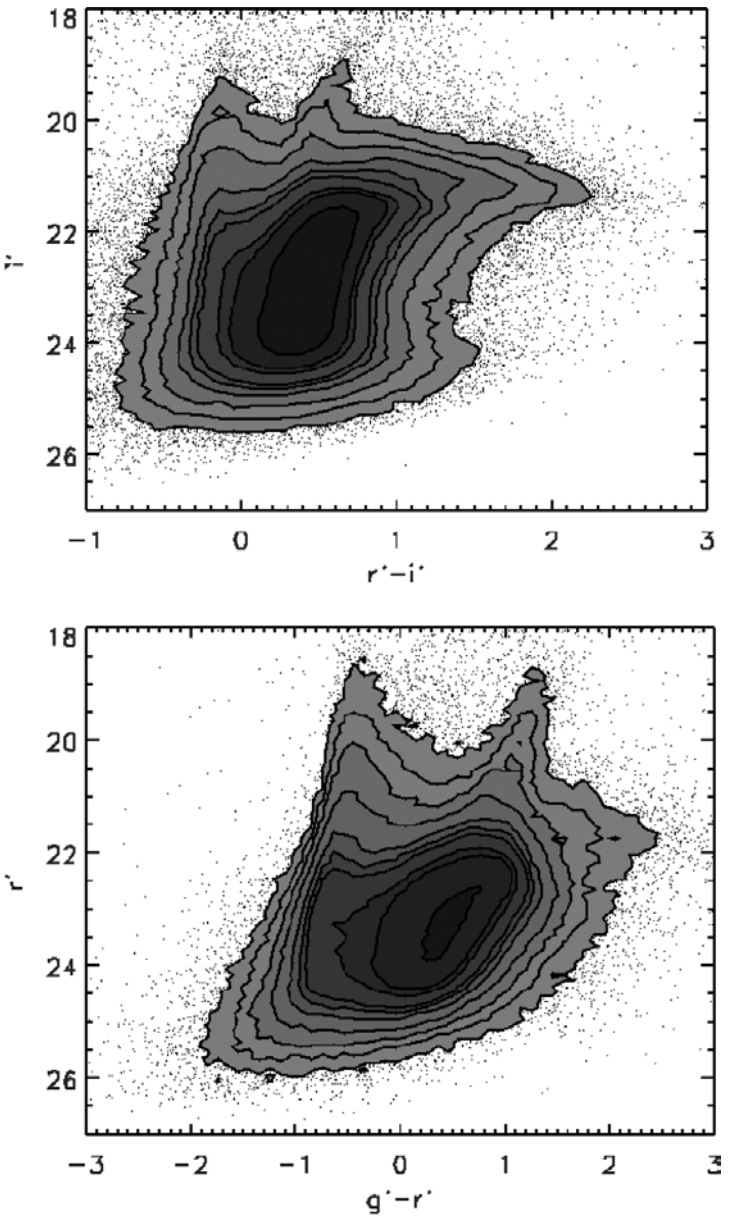

Figure 1. Isodensity contour plot (Hess diagram) of the upper half of M33. The outermost contour corresponds to a density of 50 stars per 0.1 mag box, with a step between each of 200, while for the bottom panel the box sampling has been reduced in the innermost contours to try to see the red clump. The color–magnitude diagrams display a broad red-giant branch with the tip near $i' \sim 21$ mag and a young main sequence at $(g' - r') \sim -0.5$ mag, reaching $r' \sim 20$ mag.

We perform standard profile-fitting photometry on these images using the DAOPHOT/ ALLSTAR routines (Stetson 1994). A detailed description of how the PSFs were constructed has been presented in Sarajedini *et al.* (2006). Appropriate aperture corrections were added to obtain the instrumental magnitudes. These magnitudes have been calibrated to the SDSS system by applying the transformations provided by the ELIXIR pipeline.

https://doi.org/10.1017/S1743921309991943 Published online by Cambridge University Press

The integrated magnitudes and colors of our list of candidate clusters have been calculated using the aperture-photometry routines in DAOPHOT (Stetson 1987). To be consistent with previous authors, we adopted an aperture radius of 2.2″ for the magnitude measurements and 1.5″ for the colors. Once again, these magnitudes have been calibrated to the SDSS system based on the ELIXIR transformation.

3. Candidate clusters: testing the catalog

Our detection method is based on the fact that at the distance of M33, nonstellar objects are expected to be more extended than the PSF. After subtracting the stellar PSF from all sources in our frames, extended objects leave a doughnut-shaped appearance, as they are undersubtracted in the wings and oversubtracted in the center. After visual inspection of the residual images and analysis of the FWHM, this technique leaves us with a total of 2998 extended objects: 811 candidate clusters, 1969 galaxies and 218 unknown objects. An additional rejection method based on ellipticity will be applied. Figure 2 shows the photometric properties of the final sample.

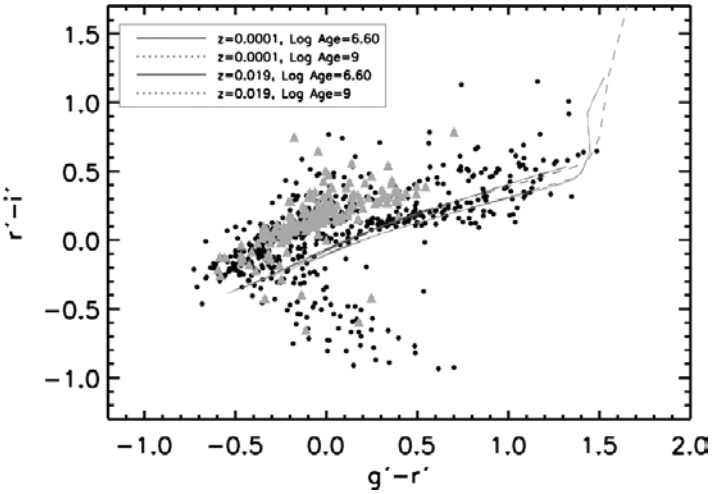

Figure 2. Color–magnitude diagram of our stellar candidate clusters (black circles) compared with the known star clusters in the SM catalog (green circles). Overplotted are single stellar population models from Girardi *et al.* (2002).

The 12 *HST*/ACS fields examined in San Roman *et al.* (2009) included 72 of the candidate clusters in the present catalog, of which 51 turned out to be genuine star clusters. This suggests that around $\sim 70\%$ of our 811 proposed candidates will be actual stellar clusters. However, from the 349 guaranteed clusters listed in the updated SM, our catalog only recovers 210 objects, implying missing objects mostly in the center of the galaxy. This is not surprising since the method is less effective in extremely crowded regions.

Comparison with the similar study of ZKH reveals unexpected discrepancies. From the total 1752 common objects between both catalogs, only 124 sources were classified as candidate clusters by both authors. As San Roman *et al.* (2009) argue, the total 'true' cluster candidates in the ZKH catalog would not be greater than $\sim 40\%$. This suggests a systematic misidentification in the candidate-object pattern or a defective PSF sustraction. Figure 3 shows the photometric differences between the two studies, which are not statistically significant.

https://doi.org/10.1017/S1743921309991943 Published online by Cambridge University Press

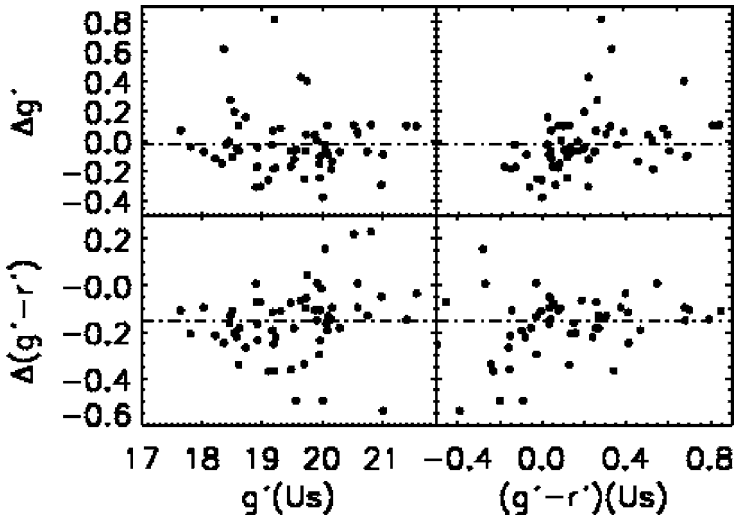

Figure 3. Comparison of the integrated photometry of common candidate clusters between the present study and ZKH. The dashed lines represent the mean differences of $\langle \Delta g' \rangle = -0.035 \pm 0.032$ and $\langle \Delta(g' - r') \rangle = -0.171 \pm 0.019$ mag, where the uncertainties are standard errors of the mean.

Acknowledgements

We gratefully acknowledge support from the US National Science Foundation through grant AST-0707277.

References

Sarajedini, A., Barker, M. K., Geisler, D., Harding, P., & Schommer, R. 2006, *AJ*, 132, 1361
Sarajedini, A. & Mancone, C. L. 2007, *AJ*, 134, 447 (SM)
San Roman, I., Sarajedini, A., Garnett, D. R., & Holtzman, J. A. 2009, *ApJ*, 699, 839
Zloczewski, K., Kaluzny, J., & Hartman, J. 2008 *AcA*, 58, 23. (ZKH)